Erschienen in: Chemical Communications : ChemComm ; 53 (2017), 35. - S. 4811-4814
https://dx.doi.org/10.1039/c7cc01342f

Synthesis of calcium carbonate in trace water environments†

Giulia Magnabosco,[a] Iryna Polishchuk,[b] Boaz Pokroy,[b] Rose Rosenberg,[c] Helmut Cölfen[c] and Giuseppe Falini *[a]

Calcium carbonate ($CaCO_3$) was synthesized from diverse water-free alcohol solutions, resulting in the formation of vaterite and calcite precipitates, or stable particle suspensions, with the dimensions and morphologies depending upon the conditions used. The obtained results shed light on the importance of solvation during crystallization of $CaCO_3$ and open a novel synthetic route for its precipitation in organic solvents.

The study of the $CaCO_3$ precipitation process is a key point for many different fields, from materials science[1–3] to biomineralization.[4–6] The processes occurring *in vivo* are of great significance even for developing new methodologies that can be applied *in vitro*.[7,8] Although it is well known that organic molecules,[9–14] supersaturation, pH, templates and temperature[15–18] play a fundamental role in the control of the polymorphism, morphology and dimension of the crystals, the hydration sphere of the involved ions is also of crucial importance.[19,20] In fact, water molecules influence strongly the reactions taking place during the $CaCO_3$ precipitation,[21] in particular the ones involved in the carbonate speciation. Few works have been done to investigate the role of the solvent during $CaCO_3$ crystallization, principally because of the difficulties in finding an appropriate solvent in which to perform the precipitation process. The ideal solvent must be able to dissolve salts and easily stay anhydrous. Among organic solvents, alcohols meet these requirements and, moreover, ethanol is the most common used in the studies present in the literature.[22–26]

When ethanol is present as an additive in an aqueous solution during a $CaCO_3$ precipitation process, it stabilizes vaterite and prevents its conversion to calcite.[26–28] In addition, Sand *et al.*[29] showed how different alcohols, their concentration and the experimental parameters affect the stability, morphology and polymorphism of $CaCO_3$ in binary alcohol–water systems, developing a model that is able to predict the outcome of the reaction based on the conditions used. When ethanol acts as a solvent, amorphous calcium carbonate (ACC) is the predominant polymorph obtained with the diffusion of ammonium carbonate into a solution of calcium chloride,[19] while using calcium hydroxide as the starting material, a mixture of calcite, vaterite and aragonite is obtained.[24] In these reactions the formation of carbonate ions from diffusing gases (*i.e.* NH_3 and CO_2) implies the presence of water. To the best of our knowledge, no reports describing direct mixing of calcium and carbonate ions in an almost water free environment are present in the literature.

In this communication we describe a new simple method to precipitate calcium carbonate from alcohol solutions of anhydrous calcium chloride and ammonium carbonate. In this system the low quantity of water diminishes the rate of carbonate speciation, favoring the precipitation of only two products, $CaCO_3$ and ammonium chloride (NH_4Cl). The effect of different molecular weight (MW) alcohols, their volume ratio and the concentration of calcium and carbonate ions (as reported in Table 1) was investigated.

Anhydrous calcium chloride and ammonium carbonate were dissolved in absolute ethanol, and then the solutions were added to absolute ethanol, or other alcohols, using syringe pumps under continuous magnetic stirring until the desired concentration was reached (see the Experimental section in the ESI†).

After 3 hours from the beginning of the reaction, only some samples produced $CaCO_3$ particles that could be separated by centrifugation at 4500*g* (italicised in Table 1). The other solutions presented a suspension of $CaCO_3$.

No other reaction times were analysed, since the goal of this communication was to investigate the precipitation of $CaCO_3$ in the absence of water in diverse organic solvents, after a time when different behaviours were detectable. Shorter reaction times resulted in a general formation of suspensions and longer

[a] *Dipartimento di Chimica "Giacomo Ciamician", Alma Mater Studiorum Università di Bologna, via F. Selmi 2, 40126 Bologna, Italy. E-mail: Giuseppe.falini@unibo.it*
[b] *Department of Material Sciences and Engineering and the Russel Berrie Nanotechnology Institute Technion-Israel Institute of Technology, 32000 Haifa, Israel*
[c] *Department of Chemistry, Physical Chemistry, Universitaï Konstanz, Universitaïstrasse 10, Konstanz D-78457, Germany*

† Electronic supplementary information (ESI) available: Experimental methods and additional characterization studies.

Table 1 Concentrations and solvents examined in this work. The solvents used were methanol (MeOH), ethanol (EtOH), 1-propanol (1-PropOH) and 1-butanol (1-ButOH). Samples prepared using 1-PropOH and 10 mM salts precipitated after 5 days (see the Experimental section in the ESI and Table S1). The samples italicised show precipitates, while the roman ones are stable dispersions

Solvent conc.	MeOH	EtOH	1-PropOH	1-BuOH
33 mM	*66% EtOH 33% MeOH*	*100% EtOH*	*66% EtOH 33% 1-PropOH*	*66% EtOH 33% 1-BuOH*
20 mM	40% EtOH 60% MeOH	*100% EtOH*	*40% EtOH 60% 1-PropOH*	*40% EtOH 60% 1-BuOH*
10 mM	20% EtOH 80% MeOH	100% EtOH	*20% EtOH 80% 1-PropOH*	*20% EtOH 80% 1-BuOH*
5 mM	10% EtOH 90% MeOH	100% EtOH	10% EtOH 90% 1-PropOH	10% EtOH 90% 1-BuOH

ones in the general formation of precipitates. In further research the time-evolution of the $CaCO_3$ formation will be studied.

The suspensions which did not show macroscopic precipitates were investigated by dynamic light scattering (DLS) and Analytical Ultracentrifugation (AUC). At 5 mM $CaCO_3$ concentration, nanoscopic species were detected by DLS for all solvents (except for methanol), at 10 mM only for methanol and ethanol and at 20 mM only for methanol (Table 2). These data indicate that with increasing solvent polarity nanoparticles can be stabilized against precipitation and that with decreasing $CaCO_3$ concentration the particle size decreases. For 5 mM and 10 mM $CaCO_3$ in ethanol and 5 mM in 1-butanol, the particle size distributions could be determined by AUC, which were in good agreement with the DLS data and showed that the 5 mM samples were rather monodisperse (Fig. S1, ESI†). However, the 5 mM and 20 mM $CaCO_3$ samples in methanol and 5 mM and 10 mM in ethanol as well as the 5 mM sample in 1-propanol contained very small species. Their sedimentation coefficients are shown in Fig. S2 (ESI†). The sedimentation coefficients are in the order of 0.1–0.3 S which is typical for ions/ion pairs with the exception of the 1-propanol sample.[30] A larger species is also detected with sedimentation coefficients of around 1 S, which falls into the range of prenucleation clusters with the exception of the 1-propanol sample.[30] Partly, even larger species with sedimentation coefficients around 3 S are observed (Fig. S2, ESI†). What these species are cannot be determined from these data. Therefore, we employed the diffusion coefficients, which can at least qualitatively be determined *via* fitting of the sedimentation raw data using the Lamm

Table 2 Measurements of particles (nm) present in the solution still stable after centrifugation at 4500*g* for 10 minutes obtained using DLS. For the sample prepared using 5 mM salts in MeOH, it was not possible to measure particles since their concentration was too low

Solvent conc.	MeOH	EtOH	1-PropOH	1-BuOH
20 mM	120.9 ± 0.73	—	—	—
10 mM	74.7 ± 0.1	65.7 ± 0.31	—	—
5 mM	—[a]	35.7 ± 0.1	117.1 ± 0.32	22.0 ± 0.3

[a] Not measurable.

Table 3 Particle diameters (d) in nm and densities (ρ) in g ml^{-1} of small species detected *via* AUC. The subscripts 1–3 indicate families of particles having different diameters and densities

	d_1/ρ_1	d_2/ρ_2	d_3/ρ_3
MeOH 20 mM	1.3/0.88	2.9/0.86	
EtOH 10 mM	1.0/1.18	2.9/1.24	7.4/0.91
EtOH 5 mM	0.9/1.29	1.8/1.48	

equation (Fig. S2, ESI†). The particle diameters (d) could be calculated applying the Stokes–Einstein equation. With a modified Svedberg equation (1), the density of the species can be estimated from the size and sedimentation coefficient as shown in Table 3.

$$\rho_i = \rho_0 + \frac{180\eta_0 s}{d^2} \quad (1)$$

where ρ_i (in g ml^{-1}) is the density of the sedimenting particles, ρ_0 and η_0 (in Poise) are the density and the viscosity of solvent, s (in Svedberg) is the sedimentation coefficient and d (in nm) is the particle size (Stokes-equivalent sphere diameter).[31]

From Table 3, it can be seen that at least for methanol and ethanol, very small species could be detected with sizes around 1 nm for the smallest species 1, 2–3 nm for species 2 and 7.5 nm for species 3. The density of the species in methanol is markedly smaller than that in ethanol although the density of the solvents is almost equal (0.79 g ml^{-1}). This indicates a higher degree of solvation of the ionic calcium and carbonate species for the more polar methanol as compared to ethanol. The smallest detected species with a size of 0.9–1.3 nm could potentially be related to a solvated $CaCO_3$ ion pair (rCa^{2+} = 0.10 nm, rCO_3^{2-} = 0.18 nm), while the larger species must already contain dozens of ions with a size similarity to prenucleation clusters for the water case.[30] The solubility of $CaCO_3$ in alcohol decreases with the increase of the alcohol MW, resulting in a higher $CaCO_3$ precipitation yield in high MW solvents even at lower starting salt concentration. The precipitates were characterized as collected after centrifugation and drying at 60 °C. No water washing was carried out to avoid any dissolution, and eventually, a re-precipitation process. The solid products were analysed by Fourier transform infrared (FTIR) spectroscopy, scanning electron microscopy (SEM) and synchrotron high resolution powder X-ray diffraction (HRPXRD). The FTIR and HRPXRD data showed that $CaCO_3$ co-precipitated with NH_4Cl, as a side product. The bands in the FTIR spectra at 1475 cm^{-1}, 876 cm^{-1} and 746 cm^{-1} (Fig. 1) correspond to ν_3, ν_2 and ν_4, respectively, vibration modes of vaterite. The bands at 1420 cm^{-1} and 712 cm^{-1} indicate the presence of calcite traces in some precipitates, while the one at 1403 cm^{-1} indicates NH_4Cl. The presence of vaterite, NH_4Cl and small amounts of calcite was also confirmed by the Rietveld analysis of the HRPXRD patterns (Fig. S3 and Table S2, ESI†). The co-presence of NH_4Cl was also confirmed by its sublimation after thermal treatment at 300 °C (Fig. S4, ESI†). The Rietveld analysis also showed that 1-propanol was the best solvent for the precipitation of vaterite (>99 wt%). This may suggest that in this solvent the solubility of vaterite and of potential prenucleation clusters (see AUC data) is lower with respect to other alcohols.

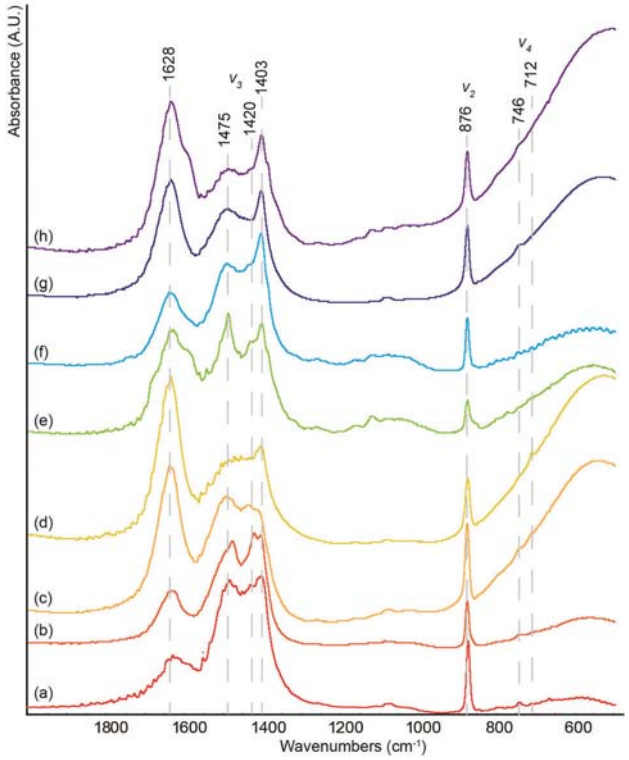

Fig. 1 FTIR spectra of samples obtained using (a) MeOH and 33 mM salts, (b) EtOH and 33 mM salts, (c) EtOH and 20 mM salts, (d) 1-PropOH and 33 mM salts, (e) 1-PropOH and 20 mM salts, (f) 1-BuOH and 33 mM salts, (g) 1-BuOH and 20 mM salts and (h) 1-BuOH and 10 mM salts.

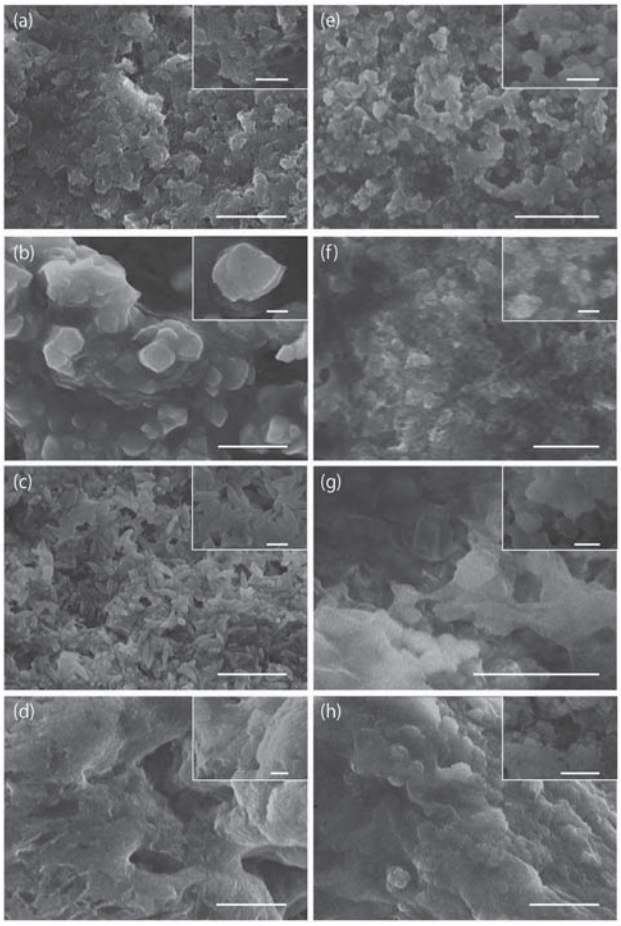

Fig. 2 SEM images of samples obtained using (a) MeOH and 33 mM salts, (b) EtOH and 33 mM salts, (c) EtOH and 20 mM salts, (d) 1-PropOH and 33 mM salts, (e) 1-PropOH and 20 mM salts, (f) 1-BuOH and 33 mM salts, (g) 1-BuOH and 20 mM salts and (h) 1-BuOH and 10 mM salts. The scale bar is 5 μm in the main picture and 1 μm in the inset.

The intensities of the band at 3000 cm^{-1} suggest a contribution of water to the ammonium absorption bands (Fig. S5, ESI†). This indication is confirmed by the thermogravimetric analysis (Fig. S4, ESI†), from which an amount of about 3–15 wt% of linked water was detected in the precipitates, according to the intensity of the absorption band at 1628 cm^{-1}.

Since after the precipitation process the quantity of water in the solution is lower than 0.5% (v/v), we can hypothesize that this water is collected from the environment due to its high affinity to the $CaCO_3$ surface and entrapped between the crystalline domains. Comparing all the samples prepared using 33 mM salt solutions it is possible to note that the intensity of the band at 1628 cm^{-1} increases with the MW of the selected alcohol. The lower solubility of water in alcohols with longer chains may promote the entrapping of water in the precipitate.

SEM imaging (Fig. 2) reveals the presence of $CaCO_3$ particles with different morphologies together with an unstructured thin layer, probably of NH_4Cl or amorphous calcium carbonate (not evident from HRPXRD and FTIR data) that covers the underlying material. The sample precipitated in the presence of methanol shows particles around 150 nm that assemble to form 3 μm aggregates with irregular shape. When the precipitation process is carried out using pure ethanol as a solvent, particles with a more regular shape are present in the samples. Using 33 mM salt concentration, pillars with hexagonal sections can be observed, while upon reducing the salt concentration to 20 mM some elongated grain-like particles form. 1-Propanol and 1-butanol precipitated samples seem to be influenced more strongly by the concentration of the salts rather than by the nature of the solvent. In fact, for both samples prepared with 33 mM salts, it is not possible to recognize any regular shape. Upon decreasing the salt concentration to 20 mM and 10 mM, some spherical particles become visible due to the reduction of the covering layer. These particles are smaller than 1 μm and have an irregular surface (Fig. 2).

These results confirm that the solvent plays a fundamental role in the crystallization of $CaCO_3$ and add new information showing that the use of different alcohols stabilizes vaterite and reduces its conversion to calcite, in agreement with previously published data.[30] The crystallization process in alcohol is slower than the one in water and, after 3 hours from ion addition, vaterite is the main component of the precipitate, while in pure water the same experimental conditions produce only pure rhombohedral calcite (Fig. S6 and S7, ESI†). However, similar to the prenucleation clusters observed in water,[30] we could also detect several very small species in methanol and ethanol, which are likely solvated ions or their clusters.

In conclusion, this simple methodology can allow the study of the interaction between $CaCO_3$ and molecules that are not

soluble in water, without the use of additional reactants, giving rise to new possible synthetic paths. Finally, the data show that the use of different solvents significantly affects the $CaCO_3$ crystallization pathway, which will be the subject of future further investigations.

We thank Dr Davide Levy for help with the analyses of the HRPXRD data. G. F. and G. M. thank Consorzio Interuniversitario di Ricerca sulla Chimica dei Metalli nei Sistemi Biologici for the support. B. P. thanks the European Research Council under the European Union's Seventh Framework Program (FP/2007–2013)/ ERC Grant Agreement (no. 336077) for the financial support and the European Synchrotron Radiation Facility for the high resolution powder X-ray diffraction measurements at beamline ID22.

Notes and references

1 L. A. Estroff and A. D. Hamilton, *Chem. Mater.*, 2001, **13**, 3227–3235.
2 D. B. Trushina, T. V. Bukreeva and M. N. Antipina, *Cryst. Growth Des.*, 2016, **16**, 1311–1319.
3 F. Nudelman and N. A. J. M. Sommerdijk, *Angew. Chem., Int. Ed.*, 2012, **51**, 6582–6596.
4 L. Addadi, A. Gal, D. Faivre, A. Scheffel and S. Weiner, *Isr. J. Chem.*, 2015, **56**, 227–241.
5 J. J. De Yoreo, P. U. P. A. Gilbert, N. A. J. M. Sommerdijk, R. L. Penn, S. Whitelam, D. Joester, H. Zhang, J. D. Rimer, A. Navrotsky, J. F. Banfield, A. F. Wallace, F. M. Michel, F. C. Meldrum, H. Cölfen and P. M. Dove, *Science*, 2015, **349**, 6760.
6 S. Weiner and L. Addadi, *Annu. Rev. Mater. Res.*, 2011, **41**, 21–40.
7 N. A. J. M. Sommerdijk and G. de With, *Chem. Rev.*, 2008, **108**, 4499–4550.
8 F. C. Meldrum and H. Cölfen, *Chem. Rev.*, 2008, **108**, 4332–4432.
9 S. Weiner and L. Addadi, *Trends Biochem. Sci.*, 1991, **16**, 252–256.
10 M. Reggi, S. Fermani, V. Landi, F. Sparla, E. Caroselli, F. Gizzi, Z. Dubinsky, O. Levy, J.-P. Cuif, Y. Dauphin, S. Goffredo and G. Falini, *Cryst. Growth Des.*, 2014, **14**, 4310–4320.
11 D. Ren, Q. Feng and X. Bourrat, *Micron*, 2011, **42**, 228–245.
12 G. Falini, S. Albeck, S. Weiner and L. Addadi, *Science*, 1996, **271**, 67–69.
13 S. Weiner and L. Addadi, *J. Mater. Chem.*, 1997, **7**, 689–702.
14 L. Kabalah-Amitai, B. Mayzel, Y. Kauffmann, A. N. Fitch, L. Bloch, P. U. P. A. Gilbert and B. Pokroy, *Science*, 2013, **340**, 454–457.
15 B. Pokroy and E. Zolotoyabko, *Chem. Commun.*, 2005, 2140–2142.
16 B. Njegić-Džakula, G. Falini, L. Brečević, Ž. Skoko and D. Kralj, *J. Colloid Interface Sci.*, 2010, **343**, 553–563.
17 J. J. De Yoreo and P. G. Vekilov, *Rev. Mineral. Geochem.*, 2003, **54**, 57–93.
18 A. Navrotsky, *Proc. Natl. Acad. Sci. U. S. A.*, 2004, **101**, 12096–12101.
19 S.-F. Chen, H. Cölfen, M. Antonietti and S.-H. Yu, *Chem. Commun.*, 2013, **49**, 9564–9566.
20 M. Sancho-Tomás, S. Fermani, M. Reggi, J. M. García-Ruiz, J. Gómez-Morales and G. Falini, *CrystEngComm*, 2016, **18**, 3265–3272.
21 F. Sebastiani, S. L. P. Wolf, B. Born, T. Q. Luong, H. Cölfen, D. Gebauer and M. Havenith, *Angew. Chem., Int. Ed.*, 2017, **56**, 490–495.
22 G. Yan, L. Wang and J. Huang, *Powder Technol.*, 2009, **192**, 58–64.
23 K. K. Sand, M. Yang, E. Makovicky, D. J. Cooke, T. Hassenkam, K. Bechgaard and S. L. S. Stipp, *Langmuir*, 2010, **26**, 15239–15247.
24 K. S. Seo, C. Han, J. H. Wee, J. K. Park and J. W. Ahn, *J. Cryst. Growth*, 2005, **276**, 680–687.
25 M. Ryu, H. Kim, J. Ahn, K. You and S. Goto, *J. Ceram. Soc. Jpn.*, 2009, **117**, 106–110.
26 Z. Zhang, B. Yang, H. Tang, X. Chen and B. Wang, *J. Mater. Sci.*, 2015, **50**, 5540–5548.
27 L. Zhang, L.-H. Yue, F. Wang and Q. Wang, *J. Phys. Chem. B*, 2008, **112**, 10668–10674.
28 F. Manoli and E. Dalas, *J. Cryst. Growth*, 2000, **218**, 359–364.
29 K. K. Sand, J. D. Rodriguez-Blanco, E. Makovicky, L. G. Benning and S. L. S. Stipp, *Cryst. Growth Des.*, 2012, **12**, 842–853.
30 D. Gebauer, A. Völkel and H. Cölfen, *Science*, 2008, **322**, 1819–1822.
31 K. L. Planken and H. Cölfen, *Nanoscale*, 2010, **2**, 1849–1869.